Comparative Electron Paramagnetic Resonance Study of Radical Intermediates in Turnip Peroxidase Isozymes[†]

Anabella Ivancich,*[,‡] Gilbert Mazza,[§] and Alain Desbois[||]

Section de Bioénérgétique and Section de Biophysique des Protéines et des Membranes, Département de Biologie Cellulaire et Moléculaire, URA 2096 CNRS, CEA Saclay, 91191 Gif-sur-Yvette, France, and CIML, UMR CNRS 6102, Parc Scientifique de Luminy, 13288 Marseille, France

Received December 13, 2000

ABSTRACT: The occurrence of isozymes in plant peroxidases is poorly understood. Turnip roots contain seven season-dependent isoperoxidases with distinct physicochemical properties. In the work presented here, multifrequency electron paramagnetic resonance spectroscopy has been used to characterize the Compound I intermediate obtained by the reaction of turnip isoperoxidases 1, 3, and 7 with hydrogen peroxide. The broad (2500 G) Compound I EPR spectrum of all three peroxidases was consistent with the formation of an exchange-coupled oxoferryl−porphyrinyl radical species. A dramatic pH dependence of the exchange interaction of the [Fe(IV)═O por$^{\bullet+}$] intermediate was observed for all three isoperoxidases and for a pH range of 4.5−7.7. This result provides substantial experimental evidence for previous proposals concerning the protein effect on the ferro- or antiferromagnetic character of the exchange coupling of Compound I based on model complexes. Turnip isoperoxidase 7 exhibited an unexpected pH effect related to the nature of the Compound I radical. At basic pH, a narrow radical species (∼50 G) was formed together with the porphyrinyl radical. The g anisotropy of the narrow radical $\Delta g = 0.0046$, obtained from the high-field (190 and 285 GHz) EPR spectrum, was that expected for tyrosyl radicals. The broad g_x edge of the Tyr$^{\bullet}$ spectrum centered at a low g_x value (2.00660) strongly argues for a hydrogen-bonded tyrosyl radical in a heterogeneous microenvironment. The relationship between tyrosyl radical formation and the higher redox potential of turnip isozyme 7, as compared to that of isozyme 1, is discussed.

The occurrence of several isozymes in plant peroxidases is widespread (*1*), but their specific physiological role is poorly understood (*2*). Recently, a differential specificity toward Mn(II) has been reported for isozyme H2 in lignin peroxidase (*3*). Turnip peroxidases (TPs)[1] are class III enzymes of the plant peroxidase superfamily (*4*). Seven isoperoxidases with distinct physicochemical properties were isolated from *Brassica napus* turnip roots. The relative proportions of turnip isoperoxidases were season-dependent (*5*). In particular, the basic (pI 11.6) isoperoxidase 7 (TP7) was only present in roots harvested during winter and represented ∼40% of the peroxidase activity. Isoperoxidase 7 was also more abundant than acidic isoperoxidases 1−3 (pI 3.5). Significant differences in the redox midpoint potentials of Compound I were measured for TP1 and TP7 (*6*). Turnip isoperoxidase 7 exhibited high oxidase activity toward indoleacetic acid (*7*). These differences in physicochemical properties and catalytic activities of turnip isozymes were attributed to subtle modifications in the protein environment of the heme active sites (*8*, *9*).

Recently, three-dimensional crystal structures of class III peroxidases belonging to the plant peroxidase superfamily have been determined at high resolution. Specifically, structural data are available for peanut (*10*), horseradish C (*11*), and barley grain (*12*) peroxidases. Although no structural data are available for turnip peroxidases, the primary sequence alignment with horseradish C indicated that the heme pocket is highly conserved (*8*, *13*, *49*). A common feature of the heme peroxidases with known three-dimensional structure is the catalytic site, which comprises a pentacoordinated heme iron with a histidine residue as the fifth ligand (*1*). Spectroscopic studies on peroxidases in the resting state have shown that the heme iron is a high-spin ferric [Fe(III)] species. Two subsequent intermediates, Compound I and Compound II, take part in the catalytic cycle. Compound I, the oxoferryl−porphyrinyl radical [Fe(IV)═O por$^{\bullet+}$] intermediate, is formed by the hydrogen peroxide-induced oxidation of the resting enzyme. In contrast, the stable radical intermediate in cytochrome *c* peroxidase originates from the oxidation of Trp 191, thus forming the catalytically active [Fe(IV)═O Trp$^{\bullet+}$] intermediate (*14*). Compound II, the oxoferryl intermediate

[†] This work was supported through the European Union HCM-Research Network (Contract FMRX-CT98-0214), the Human Frontiers Science Organization (Contract RGO349), Region Ile-de-France, CEA-Saclay, and CNRS Contract to A.I.

* To whom correspondence should be addressed: Centre d'Etudes de Saclay, Section de Bioénergétique, CNRS URA 2096, Bât 532, 91191 Gif-sur-Yvette, France. Phone: +33 1 69 08 86 57. Fax: +33 1 69 08 87 17. E-mail: ivancich@dsvidf.cea.fr.

[‡] Section de Bioénérgétique, Département de Biologie Cellulaire et Moléculaire, URA 2096 CNRS.

[§] UMR CNRS 6102.

[||] Section de Biophysique des Protéines et des Membranes, Département de Biologie Cellulaire et Moléculaire, URA 2096 CNRS.

[1] Abbreviations: TP, turnip peroxidase; TP1, TP3, and TP7, isozymes 1, 3, and 7 of turnip peroxidase, respectively; HRP C, horseradish peroxidase C; EPR, electron paramagnetic resonance; HF-EPR, high-field EPR.

10.1021/bi002826j CCC: $20.00
Published on Web 05/16/2001

[Fe(IV)═O], is formed by the one-electron reaction of Compound I with the substrate(s). A further one-electron oxidation of a second substrate molecule returns the enzyme to the resting Fe(III) state. The formation of the oxoferryl−porphyrinyl radical intermediate can be monitored by the changes in the absorption spectrum. In contrast, the formation of a protein-based radical intermediate is difficult to detect by this method since the absorption peaks of tyrosyl and tryptophanyl radicals are masked by the dominant heme bands. Alternatively, EPR and/or ENDOR spectroscopy can selectively detect either porphyrinyl or protein-based radical intermediates in heme enzymes (*15*, *16*).

EPR spectroscopy is a tool well suited for investigation of structural changes of heme active sites in enzymes and the electronic nature of the redox intermediates formed during enzyme catalysis (*17*). The protein environment of heme active sites may induce geometrical changes, which can be directly monitored by the change in *g* values observed for the heme iron EPR spectra (*18*). Moreover, EPR spectroscopy has been used to identify the nature of the Compound I intermediates in horseradish, cytochrome *c*, ascorbate, and lignin peroxidases. The use of higher magnetic fields in EPR has made it possible to resolve the *g* anisotropy of protein-based radicals in several enzymes (*19*, *50*). The accurate *g* values obtained from the high-field EPR spectra of tyrosyl radicals have been used to probe their electrostatic environment (*20*−*23*).

In this work, we have used multifrequency EPR spectroscopy to assess the electronic nature of the Compound I intermediate of three turnip isoperoxidases. The 9 GHz EPR spectra of the TP1, TP3, and TP7 isozymes treated with hydrogen peroxide were consistent with an oxoferryl moiety in exchange interaction with a porphyrinyl radical. A dramatic pH dependence of the Compound I EPR spectra was observed for the three isoperoxidases and correlated to changes in the magnetic interaction between the oxoferryl moiety and the porphyrinyl radical species. The EPR spectrum of TP7 Compound I at pH 7.7 reflected the formation of an additional narrow radical species with different relaxation properties. The high-field (285 and 190 GHz) EPR spectrum of this radical could be simulated with *g* values well within those expected for known in vitro and in vivo tyrosyl radicals (*23*, and references therein). A relationship between the redox midpoint potentials of the oxidized isozymes and the nature of the observed radical intermediate(s) is proposed and related to potential functional differences among the turnip isoperoxidases.

MATERIALS AND METHODS

Sample Preparation. Isozymes 1, 3, and 7 were purified from *B. napus* L. turnip roots (blanc dur d'hiver variety) as previously described (*5*). For the EPR measurements, the enzymes were in 100 mM Tris-HCl buffer (pH 7.7) or 100 mM acetate buffer (pH 4.5). Compound I samples were prepared by mixing manually 0.65 mM resting enzyme with a 2-fold excess of hydrogen peroxide (Aldrich), directly in the 4 mm EPR tubes kept at 0 °C. The reaction was stopped by rapid immersion of the EPR tube in liquid nitrogen, the overall procedure taking 30 s. The hydrogen peroxide concentration and the mixing time used in the experiments were those yielding the maximum Compound I intermediate, monitored by the intensity of the EPR signal.

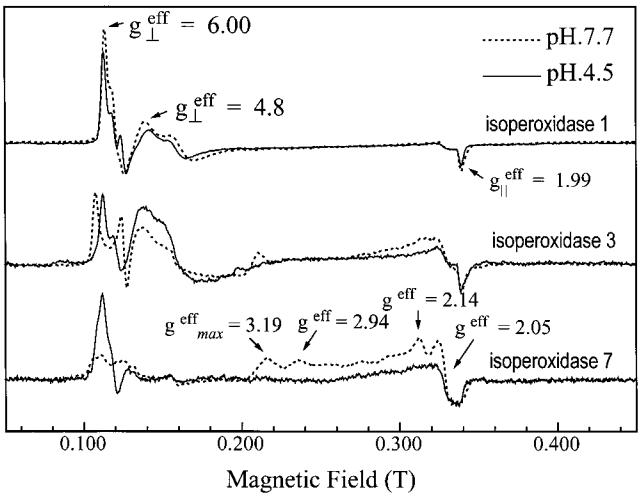

FIGURE 1: The 9 GHz EPR spectra of turnip isoperoxidases 1, 3, and 7 in the resting state, obtained for samples at pH 4.5 (—) and 7.7 (•••). Experimental conditions: temperature, 4.2 K; microwave frequency, 9.42 GHz; modulation amplitude, 4 G; modulation frequency, 100 kHz; and microwave power, 1 mW.

EPR Spectroscopy. Conventional 9 GHz EPR measurements were taken using a Bruker ER 200 spectrometer with a standard TE_{102} cavity equipped with a liquid helium cryostat (Oxford Instruments), a microwave frequency counter (Hewlett-Packard model 5350B), and an NMR gaussmeter (Bruker model ER035M). High-field EPR measurements were performed on a lab-built spectrometer described previously (*23*). The fundamental frequency (92−96 GHz) was doubled or tripled using an InP frequency doubler or tripler (Radiometric Physics, Meckenheim, Germany). The frequency was measured by using a frequency counter (EIP Microwave Inc., Milpitas, CA) with a specific accuracy of 1 kHz. Errors in *g* values were dominated by measurements in the magnetic field. The apparent *g* value of the Mn(II) MgO standard (*23*, and references therein) could be determined to within $\pm 1 \times 10^{-5}$. Consequently, the magnetic field could be calibrated to this accuracy. The reproducibility of the *g* values for a given sample was less than 5×10^{-5}. The linearity of the magnetic field sweep was no greater than that of the *g* value determination. The absolute field uncertainty was as large as 1.0 mT or about an error of 1×10^{-4} in *g* values for the measurements performed at 10 T.

Simulations of the EPR Spectra. The HF-EPR powder spectrum of the tyrosyl radical was simulated using locally written Fortran programs with standard numerical routines (*24*). The calculated spectrum was generated as previously described (*23*).

RESULTS

Figure 1 compares the 9 GHz EPR spectra of turnip isoperoxidases 1, 3, and 7 (TP1, TP3, and TP7, respectively) obtained for samples of the resting enzymes at pH 4.5 and 7.7. In all cases, axial EPR spectra with main resonances at $g_{||}^{eff} \approx 2$ and $g_{\perp}^{eff}$ between 6 and 4 were observed. Such spectra are characteristic of heme iron in the ferric [Fe(III)] high-spin and quantum-mixed spin states (*18*, *25*). In addition, a broad feature extending from 2000 to 3600 G was observed for the three isoperoxidases. This signal is attributed to two different low-spin ferric iron species,

previously reported for heme enzymes (see ref *18*). It is of note that both low-spin species are better discerned at 20 K (data not shown). One of the rhombic low-spin signals, with observed effective *g* values of 2.94, 2.10, and 1.66, has been detected previously in the spectrum of cytochrome *c* peroxidase and ascorbate peroxidases, both in their resting state (*26*, *32*). The other rhombic signal, with observed *g* values of 3.19, 2.05, and 1.28 (the third *g* value was readily observed when recording the spectra at higher temperatures), is reminiscent of the EPR spectra from different cytochromes (see ref *18*, and references therein). An increasing proportion of the low-spin signal(s) as compared to the high-spin ferric signal was observed for TP1, TP3, and TP7 ($I^{LS}_{TP7} > I^{LS}_{TP3} > I^{LS}_{TP1}$).

The nearly axial high-spin EPR signal of TP1, with observed *g* values of 6.03, 5.67, and 1.98 for g_y, g_x, and g_z, respectively, exhibited a weak pH dependence (Figure 1). In contrast, an evident pH-dependent change from axial (pH 4.5) to rhombic (pH 7.7) character was observed for the EPR signal of TP3 and TP7 (Figure 1). At pH 7.7, the effective *g* values of the TP3 rhombic signal were 6.28, 5.36, and 1.98 for g_y, g_x, and g_z, respectively. In addition, a broad feature (~300 G) centered at $g = 4.8$ was observed for isoperoxidases 1 and 3. Similar broad EPR spectra were assigned to quantum-mixed intermediate spin states in cytochrome *c′* (*27*) and model complexes (*28*). More recently, such an admixture of high-spin ($S = {}^5/_2$) and intermediate-spin ($S = {}^3/_2$) states has been invoked for soybean peroxidase (*29*). Isoperoxidase 7 showed an axial signal with *g* values and a pH dependence similar to those of TP3 (Figure 1, bottom). Two unexpected peculiarities observed for isoperoxidase 7 were the absence of an additional quantum-mixed spin signal and the marked relative conversion of the resting enzyme from the high-spin to low-spin state as a function of pH (see Figure 1, bottom).

Figure 2 shows the 9 GHz EPR spectra of the catalytic intermediates obtained by the reaction of resting turnip isoperoxidases 1 and 3 with hydrogen peroxide at pH 4.5 and 7.7. For both isoperoxidases, a broad axial signal extending over 2500 G was observed and the shape was pH-dependent. The TP1 EPR spectrum at pH 7.7 was an axial pattern with the following observed effective *g* values: $g_\perp = 2.40$ and $g_\parallel = 2.00$. At pH 4.5, the low-field edge shifted downfield ($g_\perp = 2.67$) and the narrow feature at $g_\parallel = 2.0$ became more asymmetric (see Figure 2, top). The peroxide-induced intermediate spectrum of TP3 at both pH values showed only minor differences in effective *g* values as compared to that of TP1 (see Figure 2, bottom). Unlike the signals of an isolated organic radical, the broad EPR signals were hardly observable at temperatures of >30 K (data not shown) due to relaxation broadening (*30*). Both TP1 and TP3 EPR spectra resemble the [Fe(IV)═O por$^{\bullet+}$] intermediate spectrum previously reported for *Micrococcus lysodeiktikus* (*31*) and *Proteus mirabilis* (*16*) catalases as well as for ascorbate (*32*) and lignin (*33*) peroxidases. The absorption derivative EPR spectrum was readily observed at low temperatures, although fast passage effects can be expected (*31*, *33*). For all these enzymes, the axial pattern was assigned to a porphyrinyl radical in a ferromagnetic exchange interaction with the oxoferryl heme iron.

The situation for TP7 was to some extent different (Figure 3A). The Compound I EPR spectra were essentially identical

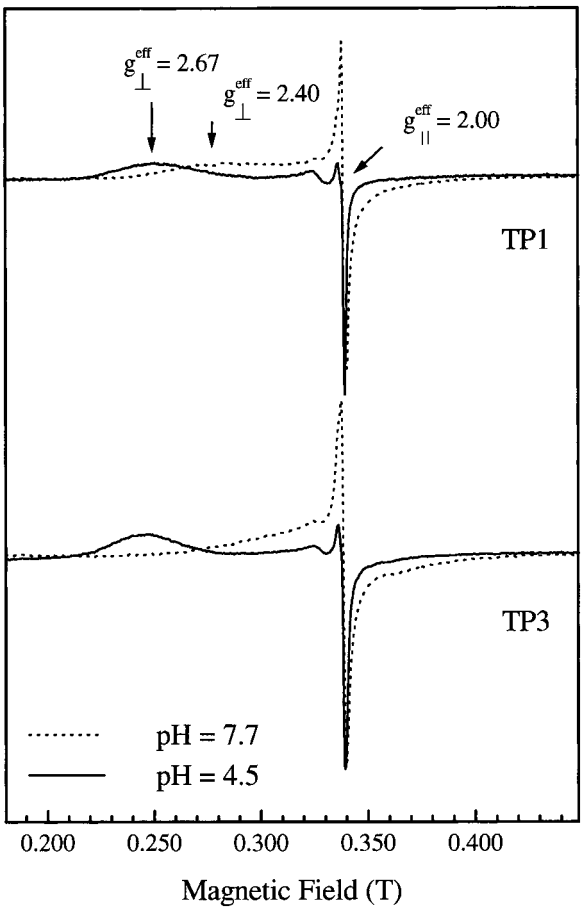

FIGURE 2: The 9 GHz EPR spectra of the Compound I intermediate [Fe(IV)═O por$^{\bullet+}$] of turnip isoperoxidases 1 and 3 (TP1 and TP3, respectively) generated by the reaction of the ferric enzymes, shown in Figure 1, with hydrogen peroxide. The experimental conditions were the same as those described in the legend of Figure 1.

to those of TP3 measured at equivalent pH values. An axial pattern with $g_\perp = 2.56$ and $g_\parallel = 2.00$ for the sample at pH 4.5 and a narrow feature at $g = 2.00$ with broad wings extending both to high and low fields were observed for the sample at pH 7.7. By contrast, an additional narrow radical where $g_{iso} = 2.0043$ could be observed at pH 7.7 (Figure 3B) when using experimental conditions for which the porphyrinyl radical intermediates of TP1 and TP3 could not be detected ($T \geq 30$ K, microwave power ≤ 50 μW). The overall breadth (50 G), the peak-to-trough width (17 G), and the saturation properties of the narrow radical were comparable to those of the tyrosyl radical intermediate in bovine liver catalase (*15*) (Figure 3B). Spin quantification of the narrow radical signal yielded 0.25 spin/heme. In addition, when using 4-fold more concentrated ferric isozyme 7 to generate Compound I, only the narrow radical signal could be detected (Figure 3A, inset). The difference in *g* values determined at the zero-crossing points of the narrow radical signal and of the $g_\parallel$ component of the por$^{\bullet+}$ (labeled pH 7.7* and pH 7.7, respectively, in the inset of Figure 3A) was the same as that previously reported for the tyrosyl and porphyrinyl radical intermediates in bovine liver catalase (*16*).

Tryptophans and tyrosines can play the role of redox-active amino acid residues in peroxidase catalysis (for a review, see ref *17*). For example, Trp 191 is the site for the radical formation of the catalytic [Fe(IV)═O Trp$^{\bullet+}$] intermediate in cytochrome *c* peroxidase (*14*). An alternative radical site for

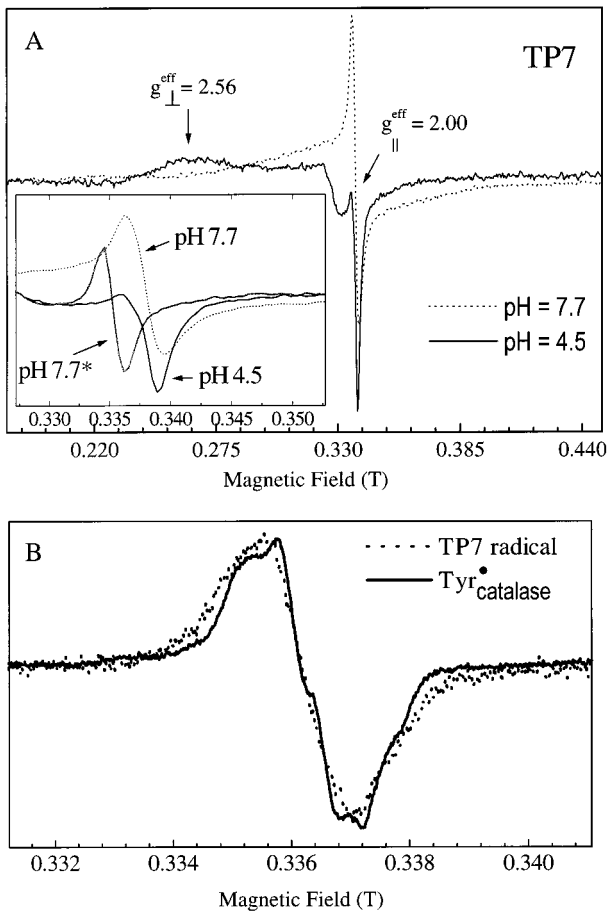

FIGURE 3: (A) The 9 GHz EPR spectra of the Compound I intermediate of turnip isoperoxidase 7 (TP7) obtained under the same conditions as those of TP1 and TP3 (see Figure 2). The inset shows the expansion of the higher-field region of the Compound I spectra ($g_{||}^{eff}$ component), together with the Compound I spectrum obtained by using a 4-fold more concentrated TP7 sample (labeled pH 7.7*). (B) The 9 GHz EPR spectrum of the TP7 radical obtained at pH 7.7 but recorded with a microwave power of 50 μW and a modulation amplitude of 0.6 G at 30 K. The tyrosyl radical intermediate of bovine liver catalase is shown for comparison.

the oxidation of veratryl alcohol has been assigned to Trp 171 in lignin peroxidase (*44*). A tyrosyl radical intermediate has been identified in the peroxidase cycle of prostaglandin H synthase (for a review, see ref *17*). Very recently, an organic radical has been observed when mixing substrate-free cytochrome $P450_{cam}$ with peroxyacetic acid. The 9 GHz EPR signal of such a radical was proposed to arise from the oxidation of a tyrosine residue (*34*). In turnip isoperoxidase 7, the overall shape of the 9 GHz EPR spectrum of the narrow radical is very similar to that of the tyrosyl radical in bovine catalase (see Figure 3B). Simulations of the 9 GHz spectrum of the TP7 narrow radical were not helpful in unequivocally assessing the nature of the radical due to the unresolved hyperfine couplings and g anisotropy.

In contrast, the high-field EPR spectrum of the TP7 radical was much more informative. The HF-EPR spectrum, recorded at 190 and 285 GHz, was dominated by g anisotropy, defined as $\Delta g = |g_x - g_z|$. The Δg value of 0.0046 was inconsistent with that of an isolated tryptophanyl radical ($\Delta g = 0.0012$; F. Lendzian, personal communication). The field positions of the three readily observed features were those expected for the intrinsic g values of a tyrosyl radical like that of the bovine catalase intermediate (see Figure 4,

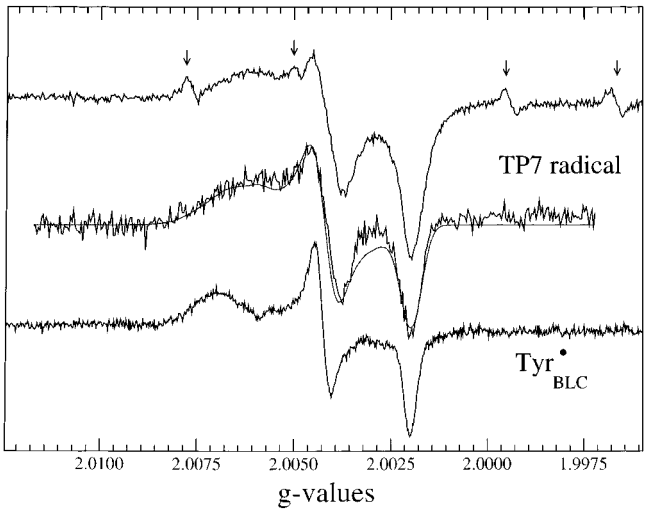

FIGURE 4: High-field EPR spectra of the narrow radical intermediate of turnip isoperoxidase 7 (TP7) formed at pH 7.7 and recorded at microwave frequencies of 190 (top) and 285 GHz (middle). Simulation of the 285 GHz spectrum is superimposed on the experimental spectrum (middle, solid gray line). Spectra were recorded at 10 K, using a field modulation of 10 G (20 G for the 285 GHz spectrum) and a frequency modulation of 30 kHz. The 285 GHz spectrum of the tyrosyl radical in bovine liver catalase ($Tyr^{\bullet}_{BLC}$), recorded at 30 K and with a field modulation of 10 G, is shown for comparison. The arrows show the lines corresponding to a Mn(II) contamination (see the text).

bottom). Moreover, the spectrum was essentially identical to the HF-EPR spectrum of the in vitro $Tyr^{\bullet}$, generated by γ-irradiation of tyrosine hydrochloride crystals (*35*). The powder pattern of the HF-EPR spectrum of the TP7 radical could be best simulated with g values of 2.0066(0), 2.0043(0), and 2.0020(8) for g_x, g_y, and g_z, respectively (see Figure 4, middle). A distribution in g_x values (with a Gaussian width of 0.00070) was necessary to account for the broad g_x component of the spectrum. Comparison of the 285 and 190 GHz EPR spectra of the TP7 radical both plotted in g values (Figure 4, top and middle) showed that the width of the three components of the **g** tensor are invariant and hence not due to hyperfine couplings. Consequently, the broad g_x component originates from an asymmetric environment of the radical. A similar low g_x value and a broad g_x component were observed in the HF-EPR spectrum of the in vitro tyrosyl radical generated by γ-irradiation of tyrosine crystals (*35*). The structural data of the tyrosine crystals indicated the presence of a strong hydrogen bond, at a distance of 1.6 Å, donated by the protonated carboxylic group of a neighboring tyrosine residue (*36*). Presumably, the presence of a positively charged amino acid residue close to the radical would have the same effect on the g_x value (*37*). Accordingly, we assign the TP7 Compound I spectrum (pH 7.7) to a tyrosyl radical in an electropositive environment. The four small lines (marked with arrows in Figure 4, top) in the 190 GHz EPR spectrum originated from a Mn(II) contamination. Two of the six hyperfine lines from the Mn(II) spectrum are outside the range shown in Figure 4. The Mn(II) lines were not observed in the 285 GHz spectrum because of thermal depopulation.

DISCUSSION

The EPR spectra of the three turnip isoperoxidases, TP1, TP3, and TP7, were typical of heme peroxidases in the

resting Fe(III) state. The EPR spectrum reflects structural features of the heme active site, and correlates to the oxidation, the spin state(s), and the coordination number of the heme iron (*18*). Accordingly, structural differences between the three isoperoxidases could be assessed. The EPR spectra of the turnip isoperoxidases allow us to conclude that TP1, TP3, and TP7 (at pH 4.3) are all high-spin hexacoordinated species. Presumably, the internal ligand is a structural water as in the case of cytochrome *c* peroxidase in solution (for a review, see ref *1*). Moreover, only TP3 at pH 7.7 exhibited an EPR spectrum consistent with a pentacoordinated heme iron. This effect is most probably due to the displacement of the structural water as a function of pH. It is of note that in the recombinant HRP C enzyme, resonance Raman (*38*) and structural data (*11*) were interpreted as arising from a high-spin pentacoordinated heme iron. In contrast, wild-type HRP C was reported to be in a mixture of penta- and hexacoordinated high-spin ferric states (*39*).

An equilibrium between high-spin only and an admixture of high- ($S = {}^5/_2$) and intermediate-spin ($S = {}^3/_2$) states was observed for isozymes 1 and 3. The resonance at $g_\perp \approx 4.8$ (Figure 1, top and middle) reflects the presence of the intermediate-spin state. Similar spectra were reported for horseradish peroxidases A2 and C2 (*25*), including a pH-dependent equilibrium between the high-spin and the quantum mixed-spin states. The absence of the $g \approx 4.8$ EPR signal for TP7 (Figure 1) indicates that all the centers are in the high-spin hexacoordinated state. Such a difference between TP7 and the other two isozymes could arise from a difference in the position of the iron atom with respect to the heme plane. Different proportions of the two different low-spin species were present in the isozymes ($I^{LS}_{TP1} < I^{LS}_{TP2} < I^{LS}_{TP7}$), with a higher content of that reminiscent of cytochromes ($g_{max} = 3.13$) in TP7 at acidic pH. Clearly, the centers with such a ligation would not react with hydrogen peroxide. The recombinant HRP C structural data revealed that the distal histidine (His 42) is 5.7 Å away from the iron atom. Our EPR data strongly suggest that in TP7 the equivalent (so-called distal) histidine residue coordinates to the sixth position of heme iron.

The Compound I EPR spectra of turnip isoperoxidases 1, 3, and 7 (and in particular those corresponding to the samples at acidic pH) were remarkably similar to that of the exchanged coupled oxoferryl−porphyrinyl radical pair that constitutes the Compound I intermediate of *M. lysodeikticus* catalase (*31*). Similar spectra were reported for lignin and ascorbate peroxidases (*32*, *33*). In all cases, the spectra were analyzed by using the model proposed by Schulz and co-workers (*40*) for horseradish peroxidase Compound I. In this model, the effective *g* values of the EPR spectrum depend on the interaction parameter (*J*), the zero-field splitting (*D*) of the oxoferryl iron, and the *g* values of the interacting species (*40*). To a first approximation, when the Zeeman energy is small compared to the zero-field splitting, the effective *g* values are given by

$$g_{||}^{\text{eff}} = g_{\text{rad}}$$

$$g_{\perp}^{\text{eff}} = g_{\text{rad}} + 2g_{\perp}^{\text{Fe}}(J/D)$$

where g_{rad} is the *g* value of the isolated porphyrinyl radical (taken to be isotropic and approximately equal to 2.0, if considering the resolution of the 9 GHz EPR spectrum), $g_\perp^{Fe}$ represents the *g* component of the oxoferryl iron [$g_\perp^{Fe} = 2.28$ and $g_{||}^{Fe} = 1.94$ (*41*)], and *D* is the zero-field splitting parameter of the oxoferryl iron. The EPR spectrum of the exchange-coupled species arises from the lowest of the three Kramers doublets, which is well separated in energy from the other two, and can be represented as an effective spin S^{eff} of ${}^1/_2$ (*42*). A thorough description of the model and its implications has been given by Hoffman and co-workers (*31*, *42*) and will not be repeated here. Recently, we have used HF-EPR combined with a more general description using an anisotropic spin−spin interaction representation to analyze the exchange-coupled oxoferryl−tryptophanyl radical intermediate in cytochrome *c* peroxidase (*35*).

The effective *g* values of the Compound I intermediate observed for TP1, TP3, and TP7 at acidic pH imply a *J*/*D* value of approximately 0.16 when using the approximation for effective *g* values shown above. Such a value implies a weaker ferromagnetic interaction compared to that of the bacterial catalase [$J/D = 0.40$ (*31*)]. The spectra of the basic pH forms of TP1, TP3, and TP7 Compound I were very similar to that of horseradish peroxidase (*40*). Accordingly, they could be explained by a weak exchange coupling ($J/D < 0.1$) with a contribution of both ferro- and antiferromagnetic interactions. A model for understanding the differences (ferro- or antiferromagnetic) in the exchange interaction of the [Fe(IV)═O por$^{\bullet+}$] intermediates of peroxidases, catalases, and model complexes has been previously proposed. A mechanism involving hydrogen bonding to the axial ligand has been invoked for the regulation of the delocalization of the unpaired electron not only over the porphyrin but also over the proximal axial ligand. Accordingly, the effect of hydrogen bonding to the proximal axial ligand would be responsible for the predominant ferromagnetic character of the exchange interaction in catalases and peroxidases (*31*, *43*). We have previously observed a subtle modification of the Compound I EPR spectrum of *P. mirabilis* catalase, which was interpreted as the effect of protonation and/or deprotonation of proximal and/or distal histidine residues (*16*). The dramatic pH-dependent changes observed in this work, for the Compound I EPR spectrum of turnip isoperoxidases, confirm and reinforce the proposal of a protein fine-tuning effect on the nature of the magnetic interaction of the oxoferryl−porphyrinyl radical pair. The correlation of the type of exchange interaction and the specific enzyme activity remains to be addressed.

Isozyme 7 was proposed to have a differential physiological role among the turnip isoperoxidases based on the physicochemical differences, such as the isoelectric point, the redox potentials of the reduced and oxidized enzyme, and the charge transfer bands in the electronic absorption spectrum (*8*). The EPR characterization of the Compound I intermediates in turnip isozymes shown in this work strongly argues for an additional peculiarity concerning the nature of the radical intermediates formed by isoperoxidase 7. At pH 4.5, an exchange-coupled oxoferryl−porphyrinyl radical species similar to those observed for TP1 and TP3 was observed for TP7. By contrast, another radical species was formed together with the porphyrinyl radical, at pH 7.7. The HF-EPR spectrum of the unexpected additional radical species of TP7 was assigned to a tyrosyl radical in a distributed electropositive environment (see the Results). An

Table 1: Environment of Candidates for the Radical Site in Turnip Isoperoxidase 7

	Tyr 233	Tyr 7	Tyr 185	Tyr 266
O_{Tyr}−Fe distance (Å)	8.4	25.6	21.7	16.6
H-bond donor(s)	Asp 247, water 855	Asp 99, water 782	water 874	none
H-bond distance (Å)	1.66 4.44	1.54 3.00	3.2	−
Lys residue	none	none	none	none
NH_{Lys}−O_{Tyr} distance	−	−	−	−
Arg residue	none	none	Arg 206	none
NH_{Arg}−O_{Tyr} distance (Å)	−	−	6.6	−

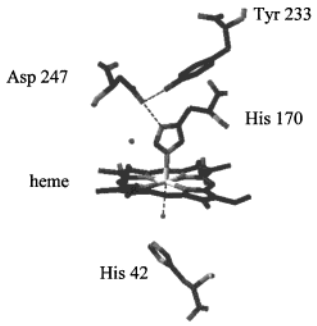

FIGURE 5: Proposed heme active site and redox-active tyrosine residue in turnip peroxidase 7, based on the crystal structure of horseradish peroxidase C (*11*) and the amino acid sequence alignment of HRP C and TP7 (*13*, *49*). Structural waters near Tyr 233 (see Table 1) and the heme iron are also represented by their oxygen atom.

equivalent situation has been reported previously for bovine liver catalase (*16*), although the formation of the tyrosyl radical was not pH-dependent in that case (*23*).

The primary structure of TP7 shows that the enzyme contains only four tyrosine residues. No crystal structure has been determined for the turnip peroxidases. Nevertheless, it is possible to use the crystal structural data of HRP C together with the sequence alignment of both enzymes (*13*, *49*) as a structural model of TP7. Such a model is useful in visualizing the purported positions and environments of the tyrosine residues. Accordingly, three such residues [Tyr 7, Tyr 185, and Phe 266, respectively (Tyr in TP7), if using the HRP C numbering] are close to the enzyme surface, hence more than 16 Å from the heme iron atom (see Table 1). Thus, if any of these three tyrosine residues is the radical site, a role as an alternative substrate binding site could be envisioned considering the recent evidence for a redox-active amino acid residue located on the enzyme surface of lignin peroxidase (*44*, *45*). A mechanism of intramolecular electron transfer between the porphyrin and the surface tryptophan residue has been proposed for lignin peroxidase (*45*). In contrast, Tyr 233 is on the proximal site and less than 10 Å from the heme iron (see Table 1). The carboxyl group of Asp 247, 1.6 Å from the phenol oxygen, could be the strong hydrogen bond donor to the tyrosyl radical with His 170 (Nϵ at 4.4 Å) playing the role of the base for deprotonation (see Figure 5). It is of note that Asp 247 is proposed to form a strong H-bond to Nδ of His 170, thus increasing the basicity of the axial ligand and helping to stabilize the [Fe(IV)═O por$^{\bullet+}$] intermediate (see, for example, refs *11* and *46*). A possible mechanism in TP7 is that Asp 247 stabilizes either the porphyrinyl radical or the tyrosyl radical, depending on the pH. An equivalent situation is observed in cytochrome *c* peroxidase involving the His 175-Asp 235-Trp 191 triad, with His 175 being the fifth ligand to the iron, Trp 191 the radical site, and Asp 235 the H-bond donor that stabilizes the tryptophanyl radical (*47*). Only partial primary sequences are available for TP1 and TP3. Hence, it is not possible to determine whether the four tyrosines of TP7 are conserved in the other isozymes. It is of note that a nonconserved tyrosine residue is not necessarily the best candidate for the radical site. The best example is the radical site in cytochrome *c* peroxidase, Trp 191; even if it is conserved in ascorbate peroxidase, the latter does not stabilize a tryptophanyl radical as catalytic intermediate but a porphyrinyl radical (*32*).

Finally, the question to address is whether such a tyrosyl radical has a specific functional role. An attractive hypothesis is that the nature of the radical intermediate (porphyrinyl or tyrosyl radical) is related to the Compound I redox potential required to oxidize specific substrates. The redox potential of the Compound I intermediate in horseradish peroxidases is approximately 1 V at pH 6.0 and it decreases by 500 mV at pH 11 (*48*). The fact that the redox potential of TP7 Compound I was reported to be 60 mV higher than that of isozyme 1 at pH 8 (*6*) may be directly related to the formation of a tyrosyl radical intermediate. Redox potentials of protein-based radical intermediates in enzymes cover a wide range of values between 0.6 and 1.3 V (for a review, see ref *17*), depending on the electrostatic environment. Taken together, these observations argue that isoperoxidase 7 is the sole turnip isozyme forming a protein-based Compound I intermediate with an oxidation potential that is higher than that of the characteristic porphyrin-based intermediate at basic pH. In addition, this isoperoxidase is expressed only in winter and, thus, could be related to specific cellular oxidative stress conditions. We propose that the observed pH-dependent nature of the radical formed in TP7 is a starting point for understanding the role of isozymes in plant peroxidases. Further experiments will be carried out to test whether substrate specificity correlates with the nature of the radical intermediates (porphyrinyl- or amino acid-based) in TP7. Moreover, to identify the tyrosyl radical site in TP7 and to clarify whether it is an alternative protein site close to the enzyme surface (Tyr 7) or to the heme active site (Tyr 233), site-directed mutagenesis and/or deuteration of the tyrosine residues in TP7 combined with HF-EPR measurements will be performed.

ACKNOWLEDGMENT

We thank Drs. Sun Un, Pierre Dorlet, and A. William Rutherford for stimulating discussions and critically reading the manuscript. We also thank one of the reviewers for the very helpful comments and remarks.

REFERENCES

1. Dunford, B. (1999) in *Heme Peroxidases*, John Willey and Sons, New York.
2. Smith, A. T., and Veitch, N. C. (1998) *Curr. Opin. Chem. Biol. 2*, 269−278.
3. Gelpke, M. D. S., Sheng, D., and Gold, M. H. (2000) *Arch. Biochem. Biophys. 381*, 16−24.
4. Welinder, K. (1992) *Curr. Opin. Struct. Biol. 2*, 388−393.
5. Mazza, G., Charles, C., Bouchet, M., Ricard, J., and Raynaud, J. (1968) *Biochim. Biophys. Acta 167*, 89−98.
6. Ricard, J., Mazza, G., and Williams, R. J. P. (1972) *Eur. J. Biochem. 28*, 566−578.

7. Job, D., and Ricard, J. (1975) *Arch. Biochem. Biophys. 170*, 527−537.
8. Welinder, K. G., and Mazza, G. (1977) *Eur. J. Biochem. 73*, 353−358.
9. Desbois, A., Mazza, G., Stetzkowski, F., and Lutz, M. (1984) *Biochim. Biophys. Acta 785*, 161−176.
10. Schuller, D. J., Ban, N., van Huystee, R. B., McPherson, A., and Poulos, T. L. (1996) *Structure 4*, 311−321.
11. Gajhede, M., Schuller, D. J., Henriksen, A., Smith, A., and Poulos, T. L. (1997) *Nat. Struct. Biol. 4*, 1032−1038.
12. Henriksen, A., Welinder, K., and Gajhede, M. (1998) *J. Biol. Chem. 273*, 2241−2248.
13. Mazza, G., and Welinder, K. G. (1980) *Eur. J. Biochem. 108*, 481−489.
14. Sivaraja, M., Goodin, D. B., Smith, M., and Hoffman, B. (1989) *Science 245*, 738−740.
15. Ivancich, A., Jouve, H. M., and Gaillard, J. (1996) *J. Am. Chem. Soc. 118*, 12852−12853.
16. Ivancich, A., Jouve, H. M., Sartor, B., and Gaillard, J. (1997) *Biochemistry 36*, 9356−9364.
17. Stubbe, J., and van der Donk, W. A. (1998) *Chem. Rev. 98*, 705−762.
18. Palmer, G. (1983) in *Iron Porphyrins*, *Part II* (Lever, A. B. P., Gray, H. B., Eds.) pp 43−88, Addison-Wesley Publishing Co., Reading, MA.
19. Burghaus, O., Plato, M., Rohrer, M., Möbius, K., MacMillan, F., and Lubitz, W. (1993) *J. Phys. Chem. 97*, 7693−7647.
20. Gerfen, G. J., Bellew, B. F., Un, S., Bollinger, J. M., Stubbe, J., Griffin, R. G., and Singel, D. J. (1993) *J. Am. Chem. Soc. 115*, 6420−6421.
21. Un, S., Atta, M., Fontecave, M., and Rutherford, A. W. (1995) *J. Am. Chem. Soc. 117*, 10713−10719.
22. Un, S., Tang, X.-S., and Diner, B. A. (1996) *Biochemistry 35*, 679−684.
23. Ivancich, A., Mattioli, T. A., and Un, S. (1999) *J. Am. Chem. Soc. 121*, 5743−5753.
24. Press, W. H., Flannery, B. P., Teukolsky, S. A., and Vetterling, W. T. (1986) *Numerical Recipes*, Cambridge University Press, New York.
25. Maltempo, M. M., Ohlsson, P. I., Paul, K. G., and Ehrenberg, A. (1979) *Biochemistry 18*, 2935−2941.
26. Yonetani, T., and Anni, H. (1987) *J. Biol. Chem. 262*, 9547−9554.
27. Fujii, S., Yoshimura, T., Kamada, H., Yamaguchi, K., Suzuki, S., Shidara, S., and Takakuwa, S. (1995) *Biochim. Biophys. Acta 1251*, 161−169.
28. Cheng, R.-J., Chen, P.-Y., Dau, P.-R., Chen, C.-C., and Peng, S.-M. (1997) *J. Am. Chem. Soc. 119*, 2563−2569.
29. Indiani, C., Feis, A., Howes, B. D., Marzocchi, M. P., and Smulevich, G. (2000) *J. Inorg. Biochem. 79*, 269−274.
30. Colvin, J. T., Rutter, R., Stapleton, H. J., and Hager, L. P. (1983) *Biophys. J. 41*, 105−108.
31. Benecky, M. J., Frew, J. E., Scowen, N., Jones, P., and Hoffman, B. M. (1993) *Biochemistry 32*, 11929−11933.
32. Patterson, W. R., Poulos, T. L., and Goodin, D. B. (1995) *Biochemistry 34*, 4342−4345.
33. Khindara, A., and Aust, S. D. (1996) *Biochemistry 35*, 13107−13111.
34. Schünemann, V., Jung, C., Trautwein, A. X., Mandon, D., and Weiss, R. (2000) *FEBS Lett. 179*, 149−154.
35. Ivancich, A., Dorlet, P., Goodin, D. B., and Un, S. (2001) *J. Am. Chem. Soc. 123*, 3048−3054.
36. Frey, M. N., Koetzle, T. F., Lehman, M. S., and Hamilton, W. C. (1973) *J. Chem. Phys. 58*, 2547−2556.
37. Un, S., Gerez, C., Elleingand, E., and Fontecave, M. (2001) *J. Am. Chem. Soc. 123*, 3048−3054.
38. Smulevich, G. (1994) *Biochemistry 33*, 7398−7407.
39. Smulevich, G., English, A. M., Martini, A. R., and Marzocchi, M. P. (1991) *Biochemistry 30*, 772−779.
40. Schulz, C. E., Devaney, P. W., Wrinkler, H., Debrunner, P. G., Doan, N., Chiang, R., Rutter, R., and Hager, L. P. (1979) *FEBS Lett. 103*, 102−105.
41. Rutter, R., Hager, L. P., Dhonau, H., Hendrich, M., Valentine, M., and Debruner, P. (1984) *Biochemistry 23*, 6809−6816.
42. Housseman, A. L., Doan, P., Goodin, D. B., and Hoffman, B. M. (1993) *Biochemistry 32*, 4430−4443.
43. Weiss, R., Mandon, D., Wolter, T., Trautwein, A., Müther, M., Bill, E., Gold, A., Jayaraj, K., and Terner, J. (1996) *J. Biol. Inorg. Chem. 1*, 377−383.
44. Doyle, W. A., Blodig, W., Veitch, N. C., Piontek, K., and Smith, A. (1998) *Biochemistry 37*, 15097−15105.
45. Blodig, W., Smith, A. T., Winterhalter, K., and Piontek, K. (1999) *Arch. Biochem. Biophys. 370*, 86−92.
46. Yamaguchi, K., Watanabe, Y., and Morishima, I. (1991) *J. Am. Chem. Soc. 113*, 4058−4065.
47. Poulos, T. L., and Kraut, J. (1980) *J. Biol. Chem. 255*, 575−580.
48. Hayashi, Y., and Yamazaki, I. (1979) *J. Biol. Chem. 254*, 9101−9106.
49. Welinder, K. (1985) *Eur. J. Biochem. 151*, 497−505.
50. Knüpling, M., Törring, J. T., and Un, S. (1997) *Chem. Phys. 219*, 291−304.

BI002826J